Acta Crystallographica Section F
Structural Biology and Crystallization Communications
ISSN 1744-3091

Structure of the ligand-binding domain of rat VDR in complex with the nonsecosteroidal vitamin D_3 analogue YR301

Shinji Kakuda,[a]* Kazuhisa Okada,[a] Hiroshi Eguchi,[a] Kazuya Takenouchi,[a] Wataru Hakamata,[b] Masaaki Kurihara[b] and Midori Takimoto-Kamimura[a]

[a]Teijin Institute for Biomedical Research, Japan, and [b]Division of Organic Chemistry, National Institute of Health Sciences, Japan

Correspondence e-mail: s.kakuda@teijin.co.jp

Received 16 May 2008
Accepted 19 August 2008

PDB Reference: vitamin D receptor ligand-binding domain–YR301 complex, 2zfx, r2zfxsf.

Vitamin D receptor (VDR) is a ligand-inducible hormone receptor that mediates $1\alpha,25(OH)_2D_3$ action, regulating calcium and phosphate metabolism, induces potent cell differentiation activity and has immunosuppressive effects. Analogues of $1\alpha,25(OH)_2D_3$ have been used clinically for some years. However, the risk of potential side effects limits the use of these substances. LG190178 is a novel nonsecosteroidal ligand for VDR. (2*S*)-3-[4-(3-{4-[(2*R*)-2-hydroxy-3,3-dimethylbutoxy]-3-methylphenyl}pentan-3-yl)-2-methylphenoxy] propane-1,2-diol (YR301) is the only one of the four evaluated stereoisomers of LG190178 to have strong activity. To understand the strong activity of YR301, the crystal structure of YR301 complexed with the rat VDR ligand-binding domain (VDR LBD) was solved at 2.0 Å resolution and compared with the structure of the VDR LBD–$1\alpha,25(OH)_2D_3$ complex. YR301 and $1\alpha,25(OH)_2D_3$ share the same position and the diethylmethyl group occupies a similar space to the *C* and *D* rings of $1\alpha,25(OH)_2D_3$. YR301 has two characteristic hydroxyl groups which contribute to its potent activity. The first is 2′-OH, which forms hydrogen bonds to the NE2 atoms of both His301 and His393. The other is 2-OH, which interacts with Ser233 OG and Arg270 NH1. These two hydroxyl groups of YR301 correspond exactly to 25-OH and 1-OH, respectively, of $1\alpha,25(OH)_2D_3$. The terminal hydroxyl group (3-OH) of YR301 is directly hydrogen bonded to Arg270 and also interacts indirectly with Tyr232 OH and the backbone NH of Asp144 *via* water molecules. Additional derivatization of the terminal hydroxyl group using the positions of the water molecules might be useful for the design of more potent compounds.

1. Introduction

The vitamin D receptor (VDR) is a member of the nuclear receptor superfamily, with which it shares structural and functional similarity (Mangelsdorf *et al.*, 1995). It contains three principal domains, a variable N-terminal domain that contains a ligand-independent activation function, a central highly conserved DNA-binding domain and a large C-terminal ligand-binding domain (VDR LBD), and a short linker between the DNA-binding domain and the VDR LBD. VDR is a ligand-dependent transcriptional regulator that acts in several physiological processes and is an important target for a wide spectrum of clinical applications such as osteoporosis, psoriasis and secondary hyperparathyroidism.

The function of VDR is regulated by the binding of vitamin D, $1\alpha,25(OH)_2D_3$, which induces a conformational change of LBD that allows the recruitment of a coactivator from the p160 (Kalkhoven *et al.*, 1998) or the DRIP/TRAP (Rachez *et al.*, 1999) families. $1\alpha,25(OH)_2D_3$ regulates calcium and phosphate metabolism, induces potent cell differentiation activity and has immunosuppressive effects (Bouillon *et al.*, 1995; Lieberherr, 1987; Hendy *et al.*, 2006). Most analogues of $1\alpha,25(OH)_2D_3$ have been synthesized with the goal of improving the biological profile of the natural ligand in order to decrease its hypercalcaemic effects for therapeutic application (Stein & Wark, 2003).

Vitamin D_3 analogues can be classified as steroidal and nonsteroidal based on their structures. The endogenous $1\alpha,25(OH)_2D_3$ and modified analogues have some shortcomings that limit their general use, mainly their potential for side effects and their mode of admini-

stration (Mizwicki & Norman, 2003). Nonsecosteroidal vitamin D_3 analogues have been under investigation for many years.

YR301 is a member of a novel class of VDR ligands that have the potential to provide improved therapeutic benefits while reducing the risk of side effects. In *in vitro* transcriptional assays and VDR affinity assays, only the (2*S*,2′*R*)-isomer (YR301) exhibited potent transcriptional activity (Hakamata *et al.*, 2008). To gain further insight into the structure–activity relationships of vitamin D and to determine the basis of the observed selectivity effect on a molecular level, we solved the crystal structure of rat VDR LBD in complex with YR301. A comparison of this structure with the structure of rat VDR LBD complexed with 1α,25$(OH)_2D_3$ (Vanhooke *et al.*, 2004) provides clues to achieving tissue selectivity and obtaining more effective potential therapeutic agents.

2. Material and methods

Rat VDR LBD (residues 116–423) lacking the flexible insertion region (residues 165–207) was amplified by polymerase chain reaction technology using the appropriate primers and inserted between the *Nde*I site and the *Not*I site of pET28a (Novagen). The resulting fusion protein contained a His tag and an N-terminal thrombin cleavage site. The constructs were produced as described by Vanhooke *et al.* (2004) and were then transformed into *Escherichia coli* strain BL21 (DE3) (Novagen). Expression was carried out in LB medium containing 20 µg ml^{-1} kanamycin with 500 µ*M* isopropyl β-D-1-thiogalactopyranoside (IPTG) at 293 K for about 16 h before harvesting by centrifugation. The cell pellets were suspended in 20 m*M* Tris–HCl pH 8.0, 100 m*M* NaCl, 10% glycerol, 5 m*M* 2-mercaptoethanol (2-ME) and and were lysed by 20 mg ml^{-1} lysozyme. The fused protein was purified by affinity chromatography using an Ni-Sepharose column. The rat VDR LBD was eluted using a buffer consisting of 20 m*M* Tris–HCl pH 8.0, 10% glycerol, 100 m*M* NaCl, 5 m*M* 2-ME, 400 m*M* imidazole. Cleavage with 50 units of thrombin per millilitre was performed overnight at 277 K. After thrombin treatment, an LBD consisting of residues 116–423 with a tag remnant of sequence GSHM attached to the N-terminus was produced. The rat VDR LBD was further purified using a gel-filtration column (GE Biosciences) equilibrated with 10 m*M* Tris–HCl pH 7.0, 100 m*M* NaCl and 10 m*M* DTT (buffer I) before crystallization.

Table 1
Data-collection and refinement statistics.

Values in parentheses are for the highest resolution shell.

Space group	$P2_12_12$
Unit-cell parameters (Å)	
a	44.22
b	47.33
c	136.43
Data collection	
Beamline	PF NW12
Wavelength (Å)	1.000
Resolution (Å)	50.00–2.00
Total No. of reflections	292936
Unique reflections	20439
R_{merge}†	0.088 (0.341)
Completeness (%)	100.0 (99.7)
Multiplicity	7.7 (7.2)
Average $I/\sigma(I)$	31.2 (6.49)
Refinement statistics	
R factor‡ (%)	20.6
R_{free}‡ (%)	25.8
R.m.s. deviation from ideal values	
Bond lengths (Å)	0.017
Bond angles (°)	1.59

† $R_{merge} = \sum_{hkl}\sum_i |I_i(hkl) - \langle I(hkl)\rangle| / \sum_{hkl}\sum_i I_i(hkl)$, where $\langle I(hkl)\rangle$ is the mean intensity of *i* reflections with intensities $I_i(hkl)$ and common indices *h*, *k* and *l*. ‡ *R* factor $= \sum_{hkl} ||F_{obs}| - k|F_{calc}|| / \sum_{hkl} |F_{obs}|$, where F_{obs} and F_{calc} are the observed and calculated structure factors. R_{free} is calculated for a randomly chosen 5% of reflections and *R* factor is calculated for the remaining 95% of reflections.

YR301 was synthesized as previously described by Hakamata *et al.* (2008). Crystallization experiments were performed using the hanging-drop vapour-diffusion method. The ligands were added to aliquots of the purified protein in a fivefold molar excess. We have cocrystallized the rat VDR LBD with YR301 and a synthetic peptide containing the L*XX*LL sequence of the coactivator DRIP 205. The synthetic peptide, with amino-acid sequence KNHPMLMNLLKDN-NH_2, was added to the rat VDR LBD/YR301 in a fivefold molar excess over the protein. Crystallization conditions were similar to those used for the VDR LBD–1α,25$(OH)_2D_3$ complex crystals; 1 µl of protein solution (10 mg ml^{-1} in buffer I) was mixed with an equal

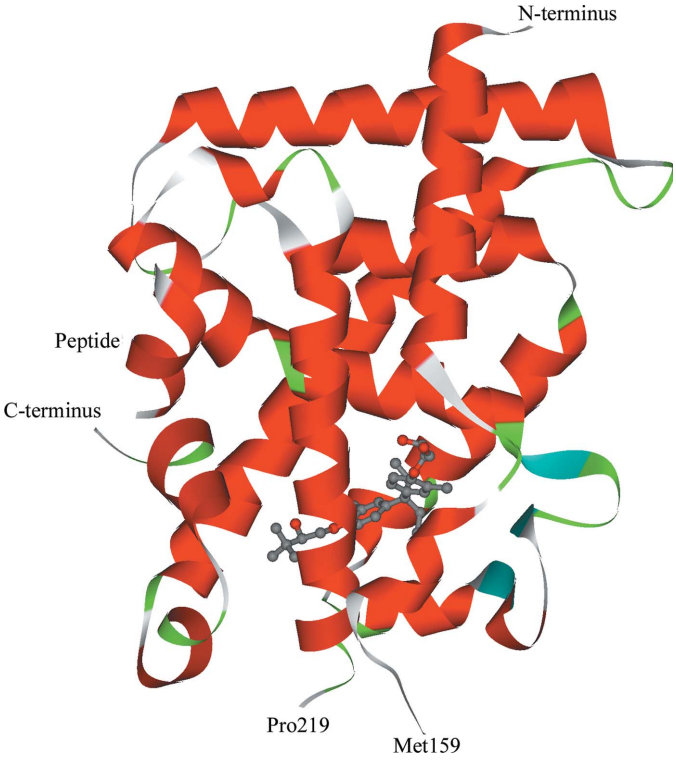

Figure 1
Overall structure of the VDR LBD–YR301 complex structure, showing the position of YR301 (shown as a ball-and-stick model).

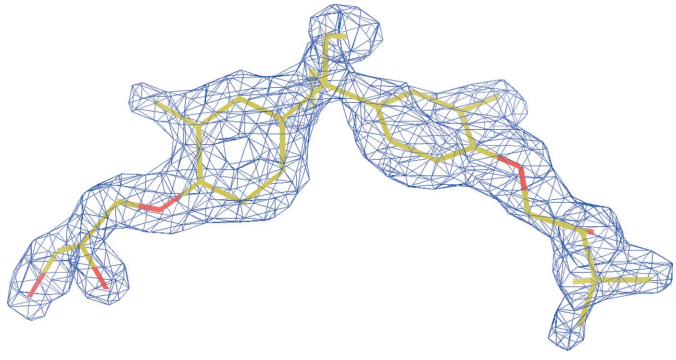

Figure 2
Conformation of the bound YR301. YR301 is shown in the $F_o - F_c$ electron-density OMIT map contoured at 1.0σ.

volume of the reservoir solution, which contained 100 m*M* MOPS pH 7.0, 200 m*M* ammonium citrate, 20% PEG 4000 and 4% 2-propanol, and equilibrated against 1 ml reservoir solution (Vanhooke *et al.*, 2004). Single crystals grew to suitable dimensions in 2–4 d. Crystals were cryoprotected in 30% glycerol and cooled at 79 K and X-ray data were collected on beamline NW12 at Photon Factory. The data were processed using the *HKL*-2000 software package (Otwinowski & Minor, 1997).

We carried out molecular replacement using *MOLREP* (Vagin & Teplyakov, 1997) from *CCP*4 (Collaborative Computational Project, Number 4, 1994) with the coordinates of the VDR LBD–1α,25(OH)$_2$D$_3$ complex [PDB code 1rk3; the solvent molecules and 1α,25(OH)$_2$D$_3$ were removed] as the initial model. Refinement was carried out using the program *REFMAC* (Murshudov *et al.*, 1997). A sample containing a random 5% of the total reflections in the data set was excluded for $R_{\rm free}$ calculations. After rigid-body refinement, electron density for 1α,25(OH)$_2$D$_3$ and the YR301 ligand was clearly constructed using *Coot* (Emsley & Cowtan, 2004). In the final refinement at 2.0 Å, the crystallographic R factor and $R_{\rm free}$ were 20.6% and 25.8%, respectively, with good stereochemistry. Statistics of the data collection and final structure are summarized in Table 1. Figures were produced using *DS Visualizer* (Accelrys; http://accelrys.co.jp/).

3. Results and discussion

The overall structure of the VDR LBD–YR301 complex is very similar to that of the VDR LBD–1α,25(OH)$_2$D$_3$ complex and we obtained a good electron-density map of the protein from Leu116 to Ser423 without the residues in the loop between 160 and 218 at 2.0 Å resolution. When compared with the VDR LBD–1α,25(OH)$_2$D$_3$ complex, the root-mean-squared deviation (r.m.s.d.) on C$^\alpha$ atoms is 1.25 Å for the VDR LBD–YR301 complex. The two protein backbones are superposable. The structure of the VDR LBD–YR301 complex and the electron density for YR301 are shown in Figs. 1 and 2, respectively.

YR301 is a nonsecosteroidal vitamin D$_3$ analogue which embeds in the ligand-binding pocket in the same position as 1α,25(OH)$_2$D$_3$ in the VDR LBD–1α,25(OH)$_2$D$_3$ complex. The chemical structures of YR301 and 1α,25(OH)$_2$D$_3$ are shown in Fig. 3. YR301 and 1α,25(OH)$_2$D$_3$ share the same position and the diethylmethyl group occupies a similar space to the *C* and *D* rings of 1α,25(OH)$_2$D$_3$, as shown in Fig. 4. The hydrophobic pocket is filled by the diethylmethyl group, which interacts with Trp282.

The interactions between the receptor and the ligand involve both hydrophobic and electrostatic contacts. A schematic representation of the interactions is shown in Fig. 5. The 2′-OH group of YR301 hydrogen bonds to His301 NE2 (2.71 Å) and His393 NE2 (2.74 Å) of VDR LBD. The 2-OH group of YR301 interacts with Ser233 OG (2.79 Å) and Arg270 NH1 (2.76 Å). In comparison, the 25-OH group of 1α,25-(OH)$_2$D$_3$ interacts with His301 NE2 (2.85 Å) and His393 NE2 (2.70 Å) and the 1-OH group interacts with Ser233 OG (2.76 Å) and Arg274 NH1 (2.83 Å). The 2′-OH and 2-OH groups of YR301 play exactly the same roles as the 25-OH and 1-OH groups of the natural ligand. Although the 3-OH group of 1α,25(OH)$_2$D$_3$ forms

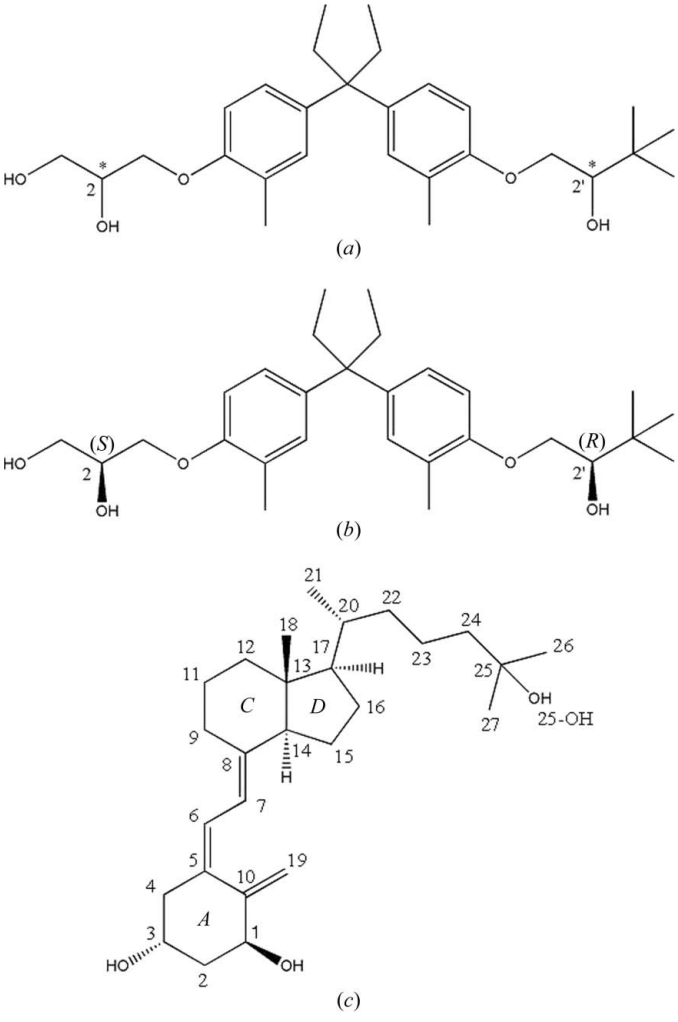

Figure 3
Chemical structures of (*a*) LG190178, (*b*) YR301 [(2*S*)-3-[4-(3-[4-[(2*R*)-2-hydroxy-3,3-dimethylbutoxy]-3-methylphenyl}pentan-3-yl)-2-methylphenoxy]propane-1,2-diol] and (*c*) 1α,25(OH)$_2$D$_3$ (1α,25-dihydroxy vitamin D$_3$).

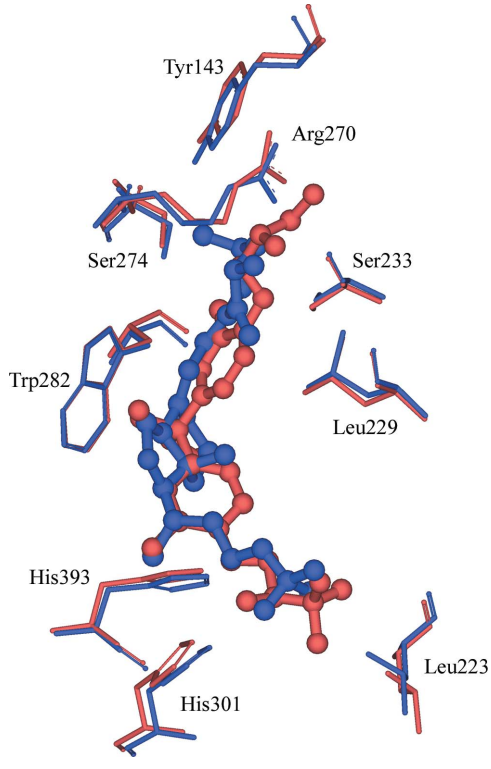

Figure 4
Ligand-binding pocket of the structure of the VDR LBD–YR301 complex superimposed on the structure of the VDR LBD–1α,25(OH)$_2$D$_3$ complex. YR301 is shown in red and 1α,25(OH)$_2$D$_3$ is shown in blue.

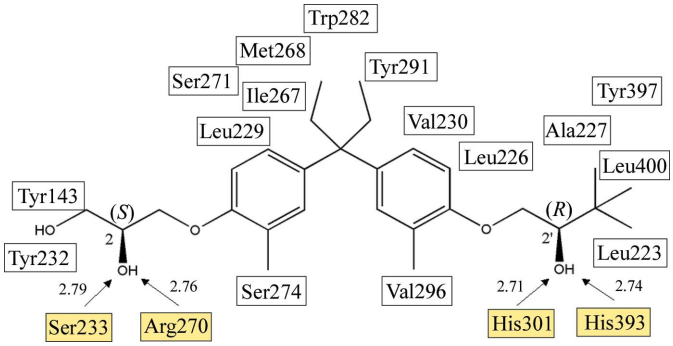

Figure 5
Schematic representation of the interactions between YR301 and VDR at a distance cutoff of 4.0 Å. Arrows correspond to hydrogen bonds between ligand and protein residues. The numbers show the distances of these hydrogen bonds in Å.

a hydrogen bond to Tyr139 OH and Ser274 OG, YR301 does not interact with those amino acids. It is probable that additional interactions with those amino acids might increase the binding affinity (Hakamata *et al.*, 2008). In the present study, we find that the terminal hydroxyl group of YR301 forms three direct hydrogen bonds to Arg270 NH1 and interacts indirectly with Tyr232 OH and Asp144 NH *via* mediated water molecules (W55, W57 and W58), despite the disorder of W57 as shown in Fig. 6. We think that the hydrogen bonds of the terminal hydroxyl groups anchor the ligands to the receptor in VDR LBD–YR301. The nonsecosteroidal vitamin D_3 analogue YR301 is a mimic of the natural ligand 1α,25(OH)$_2$D$_3$. Additional derivatization of the terminal hydroxyl group using the positions of the water molecules might be useful for the design of more potent compounds.

In this communication, we present the crystal structure of the VDR LBD–YR301 complex and compare it with the structure of the VDR LBD–1α,25(OH)$_2$D$_3$ complex. YR301 has been proven to be a selective vitamin D receptor with reduced effects on bone compared with other receptors and the structural information described here provides further details of its ligand-binding characteristics and provides some new insights into its ligand-binding requirements, which may aid in the discovery of more selective and effective potential therapeutic agents.

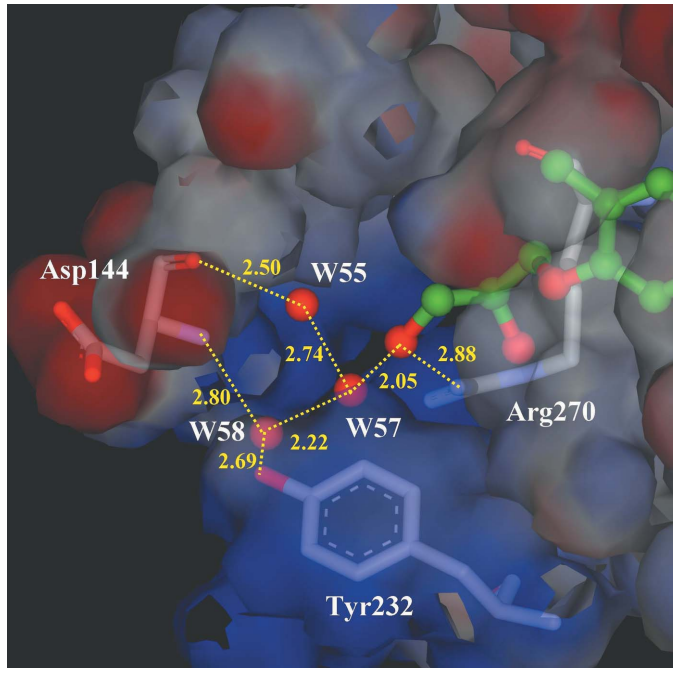

Figure 6
Interaction between the terminus of YR301 and VDR LBD. Negative charge is shown in red and positive charge in blue. The C atoms of VDR side chains are shown in grey and those of YR301 are shown in green. Hydrogen bonds are denoted by dotted lines and the numbers show their distances in Å.

References

Bouillon, R., Okamura, W. H. & Norman, A. W. (1995). *Endocr. Rev.* **16**, 200–257.
Collaborative Computational Project, Number 4 (1994). *Acta Cryst.* D**50**, 760–763.
Emsley, P. & Cowtan, K. (2004). *Acta Cryst.* D**60**, 2126–2132.
Hakamata, W., Sato, Y., Okuda, H., Honzawa, S., Saito, N., Kishimoto, S., Yamashita, A., Sugiura, T., Kittaka, A. & Kurihara, M. (2008). *Bioorg. Med. Chem. Lett.* **18**, 120–123.
Hendy, G. N., Hruska, K. A., Mathew, S. & Goltzman, D. (2006). *Kidney Int.* **69**, 218–223.
Kalkhoven, E., Valentine, J. E., Heery, D. M. & Parker, M. G. (1998). *EMBO J.* **17**, 232–243.
Lieberherr, M. (1987). *Biol. Chem.* **262**, 13168–13173.
Mangelsdorf, D. J., Thummel, C., Beato, M., Herrlich, P., Schütz, G., Umesono, K., Blumberg, B., Kastner, P., Mark, M., Chambon, P. & Evans, R. M. (1995). *Cell*, **83**, 835–839.
Mizwicki, M. T. & Norman, A. W. (2003). *J. Bone Miner. Res.* **18**, 795–806.
Murshudov, G. N., Vagin, A. A. & Dodson, E. J. (1997). *Acta Cryst.* D**53**, 240–255.
Otwinowski, Z. & Minor, W. (1997). *Methods Enzymol.* **276**, 307–326.
Rachez, C., Lemon, B. D., Suldan, Z., Bromleigh, V. & Gamble, M. (1999). *Nature (London)*, **398**, 824–828.
Stein, M. S. & Wark, J. D. (2003). *Expert Opin. Invest. Drugs.* **12**, 825–840.
Vagin, A. & Teplyakov, A. (1997). *J. Appl. Cryst.* **30**, 1022–1025.
Vanhooke, J. L., Benning, M. M., Bauer, C. B., Pike, J. W. & DeLuca, H. F. (2004). *Biochemistry*, **43**, 4101–4110.